



# A New Method for Counting Reproductive Structures in Digitized Herbarium Specimens Using Mask R-CNN

Charles C. Davis<sup>1\*</sup>, Julien Champ<sup>2</sup>, Daniel S. Park<sup>1</sup>, Ian Breckheimer<sup>1</sup>, Goia M. Lyra<sup>1,3</sup>, Junxi Xie<sup>1</sup>, Alexis Joly<sup>2\*</sup>, Dharmesh Tarapore<sup>4</sup>, Aaron M. Ellison<sup>5</sup> and Pierre Bonnet<sup>6,7</sup>

## OPEN ACCESS

### Edited by:

Yann Vitasse,  
Swiss Federal Institute for Forest,  
Snow and Landscape Research  
(WSL), Switzerland

### Reviewed by:

Dennis William Stevenson,  
New York Botanical Garden,  
United States  
Janet Prevey,  
United States Geological Survey  
(USGS), United States

### \*Correspondence:

Charles C. Davis  
cdavis@oeb.harvard.edu  
Alexis Joly  
alexis.joly@inria.fr

### Specialty section:

This article was submitted to  
Functional Plant Ecology,  
a section of the journal  
Frontiers in Plant Science

**Received:** 12 March 2020

**Accepted:** 09 July 2020

**Published:** 31 July 2020

### Citation:

Davis CC, Champ J, Park DS,  
Breckheimer I, Lyra GM, Xie J,  
Joly A, Tarapore D, Ellison AM  
and Bonnet P (2020) A New  
Method for Counting Reproductive  
Structures in Digitized Herbarium  
Specimens Using Mask R-CNN.  
Front. Plant Sci. 11:1129.  
doi: 10.3389/fpls.2020.01129

<sup>1</sup> Department of Organismic and Evolutionary Biology, Harvard University Herbaria, Harvard University, Cambridge, MA, United States, <sup>2</sup> LIRMM, Inria, University of Montpellier, Montpellier, France, <sup>3</sup> Universidade Federal da Bahia (UFBA), Salvador, Brazil, <sup>4</sup> Department of Computer Science, Boston University, Boston, MA, United States, <sup>5</sup> Harvard Forest, Harvard University, Petersham, MA, United States, <sup>6</sup> CIRAD, UMR AMAP, Montpellier, France, <sup>7</sup> AMAP, Univ Montpellier, CIRAD, CNRS, INRAE, IRD, Montpellier, France

Phenology—the timing of life-history events—is a key trait for understanding responses of organisms to climate. The digitization and online mobilization of herbarium specimens is rapidly advancing our understanding of plant phenological response to climate and climatic change. The current practice of manually harvesting data from individual specimens, however, greatly restricts our ability to scale-up data collection. Recent investigations have demonstrated that machine-learning approaches can facilitate this effort. However, present attempts have focused largely on simplistic binary coding of reproductive phenology (e.g., presence/absence of flowers). Here, we use crowd-sourced phenological data of buds, flowers, and fruits from >3,000 specimens of six common wildflower species of the eastern United States (*Anemone canadensis* L., *A. hepatica* L., *A. quinquefolia* L., *Trillium erectum* L., *T. grandiflorum* (Michx.) Salisb., and *T. undulatum* Wild.) to train models using Mask R-CNN to segment and count phenological features. A single global model was able to automate the binary coding of each of the three reproductive stages with >87% accuracy. We also successfully estimated the relative abundance of each reproductive structure on a specimen with ≥90% accuracy. Precise counting of features was also successful, but accuracy varied with phenological stage and taxon. Specifically, counting flowers was significantly less accurate than buds or fruits likely due to their morphological variability on pressed specimens. Moreover, our Mask R-CNN model provided more reliable data than non-expert crowd-sourcers but not botanical experts, highlighting the importance of high-quality human training data. Finally, we also demonstrated the transferability of our model to automated phenophase detection and counting of the three *Trillium* species, which have large and conspicuously-shaped reproductive organs. These results highlight the promise of our two-phase crowd-sourcing and machine-learning pipeline to segment and count

reproductive features of herbarium specimens, thus providing high-quality data with which to investigate plant responses to ongoing climatic change.

**Keywords:** automated regional segmentation, deep learning, digitized herbarium specimen, plant phenology, regional convolutional neural network, reproductive structures, visual data classification

## INTRODUCTION

Climate change is a potent selective force that is shifting the geographic ranges of genotypes, altering population dynamics of individual species, and reorganizing entire assemblages in all environments. A key functional trait in this regard is phenology: the timing of life-history events, such as the onset of flowering or migration. The use of museum specimens has invigorated and enriched the investigation of phenological responses to climatic change, and is one of several research directions that has brought a renewed sense of purpose and timeliness to natural history collections (Davis et al., 2015; Willis et al., 2017; Meineke et al., 2018; Meineke et al., 2019; Hedrick et al., 2020). Herbarium specimens greatly expand the historical depth, spatial scale, and species diversity of phenological observations relative to those available from field observations (Wolkovich et al., 2014). In many cases, herbarium specimens provide the only means of assessing phenological responses to climatic changes occurring over decades to centuries (Davis et al., 2015). However, a great challenge in using these specimens is accessing and rapidly assessing phenological state(s) of the world's estimated 393 million herbarium specimens (Thiers, 2017; Sweeney et al., 2018).

The ongoing digitization and online mobilization of herbarium specimens has facilitated their broad access with significant economies of scale (Sweeney et al., 2018; Nelson and Ellis, 2019; Hedrick et al., 2020) and accelerated advances in scientific investigations, including phenological assessment efforts that were underway prior to mass digitization (Primack et al., 2004; Miller-Rushing et al., 2006; Davis et al., 2015). A new vision of digitization, Digitization 2.0 (*sensu* Hedrick et al., 2020), has also sparked the integration and development of new scholarly disciplines and lines of inquiry not possible previously. Whereas Digitization 1.0 refers to the generation of digitized products from physical specimens, Digitization 2.0 is the use of natural history collections to answer scientific questions using only their digitized representation, rather than the physical specimen itself.

In recent years, scientists have used these digitized herbarium specimens in novel ways (e.g., Meineke et al., 2018; Meineke et al., 2019; Hedrick et al., 2020) and greatly increased the pace at which key phenological trait data can be harvested from tens of thousands of specimens. The platform *CrowdCurio-Thoreau's Field Notes* (Willis et al., 2017) was one of the first attempts to move beyond the standard practice of coding phenology of herbarium specimens using binary (presence/absence) coding (e.g., specimen A has flowers, specimen B has fruits: Primack et al., 2004; Miller-Rushing et al., 2006). Many of these efforts have also focused largely on flowering, ignoring other key phenophases.

Rather, users of *CrowdCurio* use a crowd-sourcing pipeline to score and quantify all phenophase features—bud, flowers, and fruits—for each specimen processed. This pipeline has facilitated the first development of ratio-based approaches to quantitatively assess the early, peak, and terminal phenophases from herbarium specimens and determine phenological changes within and between seasons (Williams et al., 2017; Love et al., 2019). The recent large-scale deployment of the *CrowdCurio* pipeline on the crowdsourcing website Amazon Mechanical Turk has demonstrated the power and scale of such fine-grained phenophasing to understand latitudinal variation in phenological responses (Park et al., 2019).

Despite the great promise of crowd-sourcing for phenophase detection, it is still time-consuming and can become cost-prohibitive to process entire collections spanning whole continents. Machine-learning approaches have the potential to open up new opportunities for phenological investigation in the era of Digitization 2.0 (Pearson et al., 2020). Recent efforts (Lorieul et al., 2019) have demonstrated that fully automated machine-learning methods—and deep learning approaches based on convolutional neural networks in particular—can determine the presence of a fruit or flower in a specimen with >90% accuracy. Convolutional neural networks were proven effective at predicting all phenophases of a specimen, based on classification of nine phenological categories. These predictions, estimated from proportions of buds, flowers and fruits, reach an accuracy (true positive rate) >43%, which is equivalent to the capability of human experts (Lorieul et al., 2019). This large-scale automated phenophase estimation, based on an annotation method developed by Pearson (2019), was tested on species belonging to a particularly difficult taxon (i.e., the Asteraceae family), for which visual analysis of numerous and tiny reproductive structures is known to be visually challenging. This work demonstrated the potential of deep learning technologies to estimate fine-grained phenophases, but further improvements are needed to support ecological investigation of diverse taxa.

Although Pearson (2019) successfully determined reproductive status (i.e., fertile vs. sterile specimens), neither the precise location (i.e., image segment) nor the number of phenofeatures present on a specimen was quantified (Lorieul et al., 2019). A quantitative machine-learning approach would have the value and impact that *CrowdCurio* has already achieved, but could be scaled-up in speed and cost-effectiveness. A recent proof-of-concept study (Goëau et al., 2020) used human-scored data to train and test a model using instance segmentation with Mask R-CNN (Masked Region-based Convolutional Neural Network: He et al., 2017) to locate and count phenological features of *Streptanthus tortuosus* Kellogg (Brassicaceae). This assessment clarified several determinants of model success for identifying and counting phenological features,

including: the type of masking applied to human annotations; and the size and type of reproductive features identified (e.g., flowering buds, flowers, immature and mature fruits). Moreover, the model was more successful identifying and counting flowers than fruits, and was applied only to a single species with relatively little human-scored training data (21 herbarium specimens). The transferability of this model to other, more distantly related species was not examined.

Here, we leverage extensive data gathered using our crowd-sourcing platform *CrowdCurio* to develop and evaluate an instance segmentation approach using Mask R-CNN to train and test a model to identify and count phenological features of a larger number of species. Specifically, we investigated digitized specimens from six common spring-flowering herbs of the eastern United States: *Anemone canadensis*, *A. hepatica*, *A. quinquefolia*, *Trillium erectum*, *T. grandiflorum*, and *T. undulatum*. As with any feature detection model, accurate human-collected data are required to train, test, and refine these models. We thus gathered phenological data from these species using *CrowdCurio* to provide expert annotation data of buds, flowers, and fruits to train and test our models. Phenological data previously collected by non-expert citizen scientists was used to further evaluate the performance of these models (Park et al., 2019). Our goals were to: (1) determine how reliably we could localize and count these features; (2) determine the accuracy in automated scoring of different phenological features; and (iii) assess the transferability of models trained on one species to other, distantly related ones.

## MATERIALS AND METHODS

### Dataset

Our experiments are based on a subset of the data used in Park et al. (2018, 2019) comprising six species in two genera of common spring-flowering herbs, *Anemone* and *Trillium*. This subset includes 3073 specimens of: *Anemone canadensis* ( $N = 108$ ), *A. hepatica* ( $N = 524$ ), *A. quinquefolia* ( $N = 686$ ), *Trillium erectum* ( $N = 862$ ), *T. grandiflorum* ( $N = 226$ ), and *T. undulatum* ( $N = 667$ ). Each specimen (herbarium sheet) was previously examined using the *CrowdCurio-Thoreau's Field Notes* platform by, on average, three citizen-scientists. For the purposes of this study, these specimens were additionally scored by expert botanists to provide the most accurate training and testing data possible. Annotators added markers in the center of each visible reproductive structure (bud, flower, or fruit), and determined its type, number, and spatial location. For our experiments, we randomly split this dataset into two parts: one ( $N = 2457$ ) for training the deep-learning models and one for testing them (*i.e.*, for evaluating their predictive performance;  $N = 615$ ).

Apart from the comparative experiment described in *Machine-Learning vs. Crowd-Sourcing* section, only the annotations of experts were used to train and test the deep-learning models. We also only used the annotations of one of the experts for each specimen (selected in a pre-defined order). The final dataset contains 7,909 reproductive structures (6,321 in

the training set and 1,588 in the test set) with the following imbalanced distribution: 492 buds (6.2%), 6,119 flowers (77.4%), and 1,298 fruits (16.4%). Fruits were counted without any knowledge of seeds.

### Deep-Learning Framework

Several deep-learning methods have been developed in recent years to count objects in images. One family of methods can be qualified as density-oriented methods (Wang et al., 2015; Zhang et al., 2015; Boominathan et al., 2016). They are usually based on U-Net architectures (Ronneberger et al., 2015) that are trained on annotations of object centers (indicated by dots) and predict density maps that are integrated to obtain counts. U-Net-based methods were developed originally for counting crowds and have been extended recently to counting cells (Falk et al., 2019) and animals (Arteta et al., 2016). The drawback of these methods is that they are better suited for cases where the density of objects in the image is high. This is not true in our case; the examined herbarium specimens averaged <3 objects per specimen, even fewer if we consider buds, flowers, and fruits separately.

Another deep-learning method is “direct counting” (*a.k.a.* “glancing”), which trains the model with the true count on the global image (e.g., Seguí et al., 2015). The main drawback of direct counting is that it cannot predict a count value that has no representative image in the training set. That is, the network is not really counting but only inferring the counts from the global content of the image. In preliminary experiments (not reported here), we found that direct-count methods tended to systematically under-estimate the true counts and have an unacceptably high variance.

The alternative method that we used in this study is to equate counting with object-detection; the counts of the object of interest are then equal to the sum up the number of detected objects. To detect buds, flowers, and fruits, we used Mask R-CNN, which is among the best-performing methods for instance segmentation tasks in computer vision (He et al., 2017). We used Facebook’s implementation of Mask R-CNN (Massa and Girshick, 2018) using the PyTorch framework (Paszke et al., 2019) with a ResNet-50 architecture (He et al., 2016) as the backbone CNN and the Feature Pyramid Networks (Lin et al., 2017) for instance segmentation. To adapt this architecture to the data in our study (see previous section), we had to address the following methodological issues:

1. *Mask computation.* The training data expected by Mask R-CNN must consist of all the objects of interest visible in the training images, each object being detected individually and associated with a segmented region (encoded in the form of a binary mask). However, the data available for our study did not fully meet these conditions as the objects were detected only by dot markers (roughly in the centre of the reproductive structure). From these dot markers, we generated dodecagons, such as the ones illustrated in **Figure 1**, which best covered the reproductive structures. To adapt the size of the dodecagons to buds, flowers, and fruits, we manually segmented five of each (selected at



**FIGURE 1** | Example of a specimen of the training set containing six reproductive structures (flowers) marked by dodecagons.

random from each genus) and calculated the average radius of the circle enclosing each structure.

2. *Input image size.* Images were resized to 1,024 pixels (long edge)  $\times$  600 pixels (short edge). This guaranteed a sufficient number of pixels for the smallest dodecagons while maintaining a reasonable training time (5–10 h per model) on a computer comparable to a mid-tier consumer device (i.e., recent GPUs with  $\pm 12$  GB of RAM).
3. *Anchor size.* Anchors are the raw rectangular regions of interest used by Mask R-CNN to select the candidate bounding boxes for mask detection. We designated their size so as to guarantee that all dodecagons had their entire area covered.

**Figure 2** Illustrates four example detections using Mask R-CNN: one with a perfectly predicted count, and three with over- or under-estimated counts. For each example, we show (a part of) the original image, the ground-truth masks (computed from expert botanist input), and the automated detections computed by the deep-learning framework.

We then trained a set of models corresponding to three distinct scenarios to be evaluated:

1. *One model per species.* In this scenario, we trained one Mask R-CNN model for each species (i.e., six models in total) to detect its buds, flowers, and fruits.
2. *One single model for all species.* In this scenario, we trained a single Mask R-CNN for all species and all types of reproductive structures (buds, flowers, fruits).
3. *Cross-species models.* Last, we assessed the transferability of models trained on some species to other ones. We trained three models on only two *Trillium* species: i.e., one on *T. erectum* and *T. grandiflorum*, one on *T. erectum* and *T. undulatum*, and one on *T. undulatum* and *T.*

*grandiflorum*. Each of these three models were then tested on the *Trillium* species not included in the training set.

## Evaluation Metrics and Statistics

We evaluated the accuracy of the models in four ways:

1. *Counting error.* The counting error  $e_{i,k}$  for a specimen  $i$  and a given type of reproductive structure  $k \in \{bud, flower, fruit\}$  was defined as the difference between the true count and the predicted count:

$$e_{i,k} = \hat{c}_{i,k} - c_{i,k} \quad (1)$$

where  $c_{i,k}$  is the true count of reproductive structures of type  $k$  in specimen  $i$  and  $k$ ,  $\hat{c}_{i,k}$  is the predicted count. Note that the counting error can be positive or negative. A detailed description of the distribution of the counting error is provided using letter-value plots (Heike et al., 2017), which provide a more comprehensive view of the statistics through a larger number of quantiles.

2. *Mean Absolute Error (MAE).* The MAE measures the overall error by averaging the absolute value of the counting error of each specimen and each type of reproductive structure:

$$MAE = \frac{1}{N} \sum_i \sum_k |e_{i,k}| \quad (2)$$

3. *Coefficient of determination ( $R^2$ ).* This statistic measures the amount of variance explained or accounted by the model:

$$R^2 = 1 - \frac{\sum_i (c_i - \hat{c}_i)^2}{\sum_i (c_i - \bar{c})^2} \quad (3)$$

where  $i$  indexes the observations and ranges from 1 to the

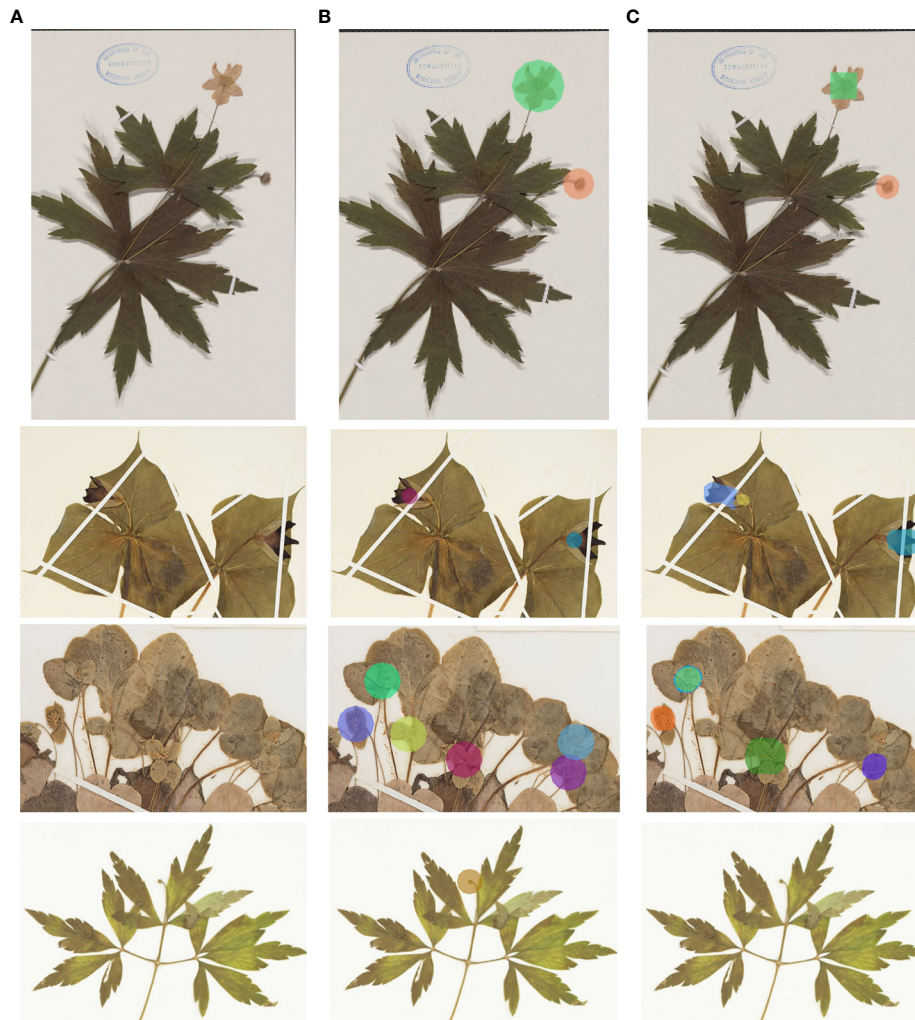


**FIGURE 2 |** Examples of detection (colors do not have a particular meaning)—(A) original image; (B) ground-truth markers; (C) automatically detected masks. The first row corresponds to a typical case with a perfect count. The second row corresponds to a case of over-estimated counts (one of the flowers was detected as two flowers). The last two rows correspond to under-estimated.

total number of observations,  $c_i$  is the observed count,  $\hat{c}_i$  is the predicted count, and  $c$  is the mean of the observed counts.

4. *Predicted counts box-plots.* A detailed description of the distribution of the predicted counts as a function of the true counts is provided using box-plots indicating median value, quartiles, variability outside quartiles, and outliers.

### Machine-Learning vs. Crowd-Sourcing

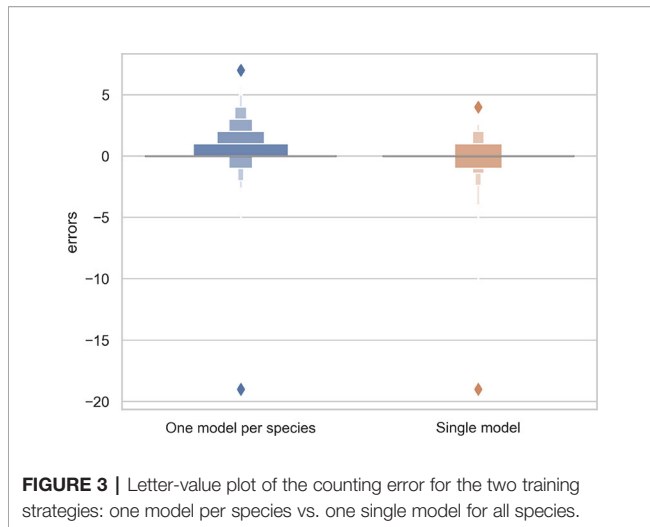
We compared the counts predicted by Mask R-CNN with those obtained when the reproductive structures on herbarium specimens were counted by crowd-sourcers (Park et al., 2019). The comparison was done on the intersection of the test sets of both studies (i.e., on 544 specimens, equal to 88% of the test set of previous experiments). These 544 specimens were annotated by 483 different annotators using Amazon Mechanical Turk. On

average, each specimen was annotated by 2.5 different crowd-sourcers.

## RESULTS

### A Single Model vs. Species-Specific Models

The  $R^2$  value for the separate training model for each species and the single model for all species was 0.70 and 0.71, respectively. Thus, the single model for all species provides marginally better results while being simpler to implement and more scalable. As shown in **Figure 3**, the main problem of single species training models is that they tend to over-predict the number of reproductive structures (number of positive errors > than number of negative errors; **Figure 3**). The

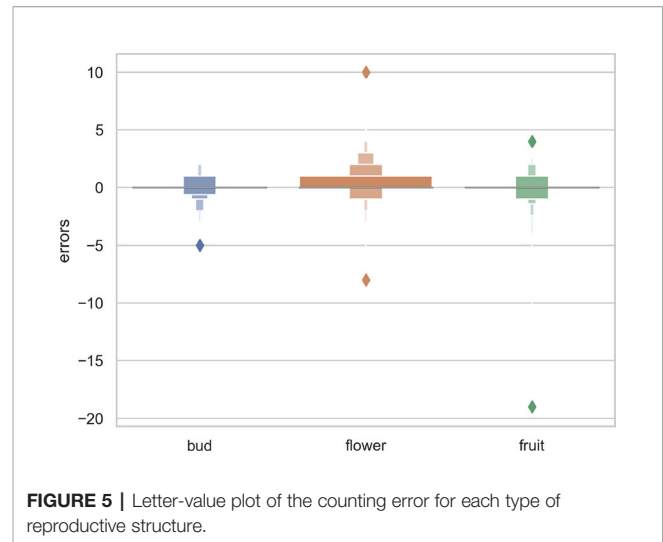


extreme outlier in **Figure 3** with a very high negative error resulted from a species being assessed by the model that had been misidentified in the collection.

The predictions of the single species training models were very accurate for  $\leq 3$  reproductive structures, whereas the single model for all species had high accuracy when  $\leq 4$  reproductive structures were present (**Figure 4**). The variance of the predicted counts was higher for specimens with more reproductive structures but the median predicted count equalled the actual count for  $\leq 7$  reproductive structures and the counting error (interquartile distance) was usually  $< 1$  structure. Specimens with  $> 8$  reproductive structures had larger errors but only accounted for 4.2% of the specimens examined.

## Distinguishing Reproductive Structures Counting Results

The overall numbers of detected reproductive structures and their relative proportions were very close to their actual values (**Table 1** and **Figure 5**). The Mean Absolute Error (MAE) was



also quite low for all types of reproductive structures, but this is due in large part to the fact that the median number of structures per phase and specimen is low. The median number of fruits and buds, in particular, is much lower than the median number of flowers. The  $R^2$  values (**Table 1**) and the box plots of the predicted counts (**Figure 6**) provide a more relevant comparison of the predictive performance for each type of structure. Flowers are the best detected structures ( $R^2 = 0.76$ ), followed by fruits ( $R^2 = 0.33$ ) and buds ( $R^2 = 0.12$ ). The lower performance for buds is due to several factors: (i) the lower number of samples in the training set—90.25% of specimens had no buds and 98.05% had  $< 3$  buds, (ii) their smaller size and (iii), their visual appearance that is less distinctive than flowers or fruits. Fruits are affected by the same factors but to a lesser extent.

## Occurrence and Dominance of Reproductive Structures

Although the model was not developed or trained to directly detect presence or absence of each reproductive structure, we

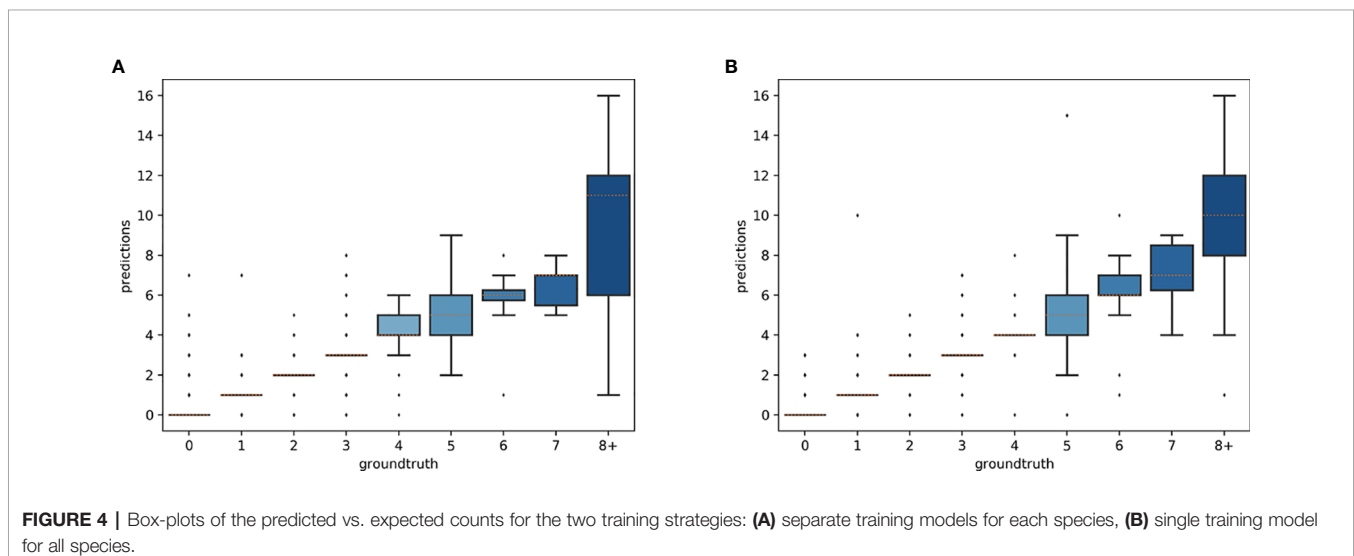


**TABLE 1** | Predicted and true counts (percent of specimens in parentheses) of buds, flowers, and fruits for all specimens pooled.

	Buds	Flowers	Fruits	All
True number of structures	107 (6.7)	1,241 (78.1)	240 (15.1)	1,588
Predicted number of structures	109 (6.1)	1,431 (80.0)	248 (13.9)	1,788
MAE	0.20	0.51	0.27	0.33
R2	0.12	0.76	0.33	0.71

were able to extrapolate the presence of each feature and which feature was most frequent on a specimen (Table 2). The detection accuracy of buds, flowers, and fruits was >87% and the accuracy of determining relative abundance of a certain organ category (e.g., number of flowers > number buds or fruits) was >90% (Table 2). Confidence in this strong result should be tempered by the actual frequency of occurrence and dominance. Observed relative presences of buds, flowers, and fruits, and dominance of fruits vs. flowers all are quite disparate. Error rates (false negatives and positives) for these all are non-zero, but are lower in all presence and dominance categories (Table 2).

### Species-Specific Models

Overall, the reproductive structures were detected more accurately for *Trillium* species than *Anemone* species (Figures 7 and 8). At the species-specific level, the  $R^2$  score was lowest for *A. canadensis* (0.01) which is the species with the least number of training samples (108 specimens). The  $R^2$  score was better for the other species and increased with the number of training samples:  $R^2 = 0.51$  for *T. grandiflorum*,  $R^2 = 0.64$  for *A. hepatica*,  $R^2 = 0.76$  for *T. undulatum*,  $R^2 = 0.85$  for *A. quinquefolia* and  $R^2 = 0.89$  for *T. erectum*. Counting errors rarely exceeded  $\pm 2$ , and the few strong outliers corresponded to very difficult cases or annotation errors. The median value of predicted counts was correct in almost all cases (Figure 7); exceptions were for *T. grandiflorum* specimens with four structures and *A. hepatica* with seven, both corresponding to instances involving a small number of specimens with large numbers of reproductive structures.

### Model Transferability

The aim of this experiment was to assess whether reproductive structures on one species could be estimated using a model

trained on a different, related species. Unsurprisingly, estimation was less accurate when the target species was not represented in the training set (Figures 9–11). However, it is still possible to count the reproductive structures of a target species based on a model trained on different species of the same genus (i.e., without any specimen of the target species in the training data). The  $R^2$  score was higher for *T. erectum* ( $R^2 = 0.72$ ; Figure 9) and *T. undulatum* ( $R^2 = 0.66$ ; Figure 10), which are morphologically more similar to one another than either is to *T. grandiflorum* ( $R^2 = 0.02$ ; Figure 11). Figures only show the results for *Trillium* but similar conclusions were obtained for *Anemone* ( $R_2$  scores respectively equal to 0.75 for *A. quinquefolia*, 0.39 for *A. hepatica* and  $-0.39$  for *A. canadensis*).

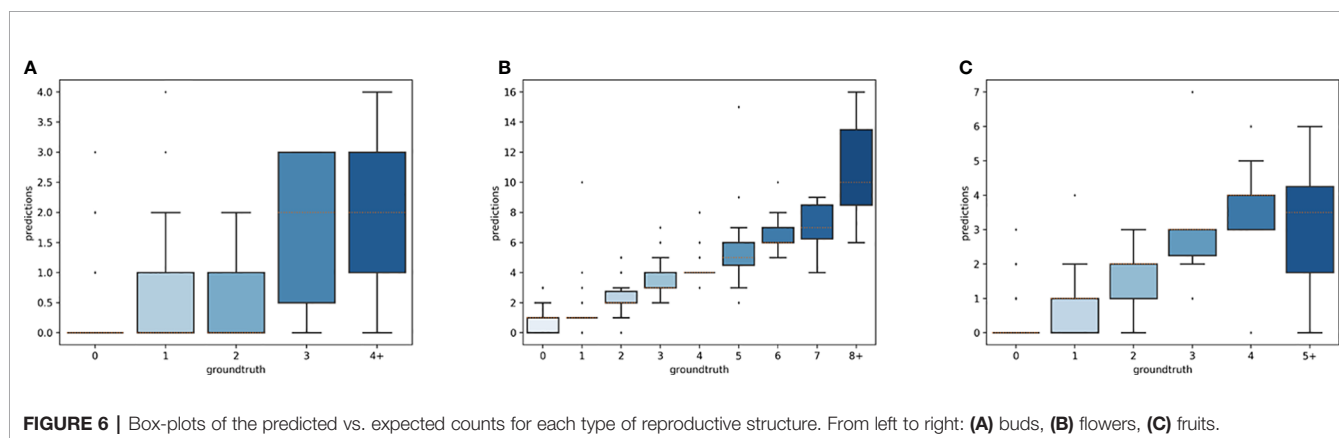
### Machine-Learning vs. Crowd-Sourcing

On average, the deep learning model had a significantly lower ( $P < 0.001$ ) MAE and better  $R^2$  score than any individual crowd-sourcer, but still an order of magnitude larger than the MAE of botanical experts (Tables 3 and 4). Interestingly, we can observe that crowd-sourcers have a much harder time detecting buds than the Mask R-CNN model. The MAE obtained by averaging the counts of the different crowd-sourcers was only marginally higher than the MAE from Mask R-CNN ( $P = 0.3$ ). Note that a counts averaging strategy could also be used for the deep learning approach, i.e., by averaging the scoring of several deep learning models. This technique is referred to as an *ensemble* of models in

**TABLE 2** | Accuracy of detection and relative dominance of buds, flowers, and fruits (data pooled for all species).

Observed	Buds	Flowers	Fruits	Flowers $\geq$ Buds	Fruits $\geq$ Flowers
	<b>9.75</b>	<b>82.92</b>	<b>20.00</b>	<b>96.09</b>	<b>21.13</b>
True positives (correctly detected)	51.66	97.25	78.86	98.98	76.15
True negatives (correctly undetected)	91.89	49.52	89.83	8.33	95.65
False positives	8.10	50.47	10.16	91.66	3.71
False negatives	48.33	2.74	21.13	1.01	23.84
Overall Accuracy	87.97	89.11	87.64	95.44	92.03

Values are percentages.

**FIGURE 6** | Box-plots of the predicted vs. expected counts for each type of reproductive structure. From left to right: (A) buds, (B) flowers, (C) fruits.

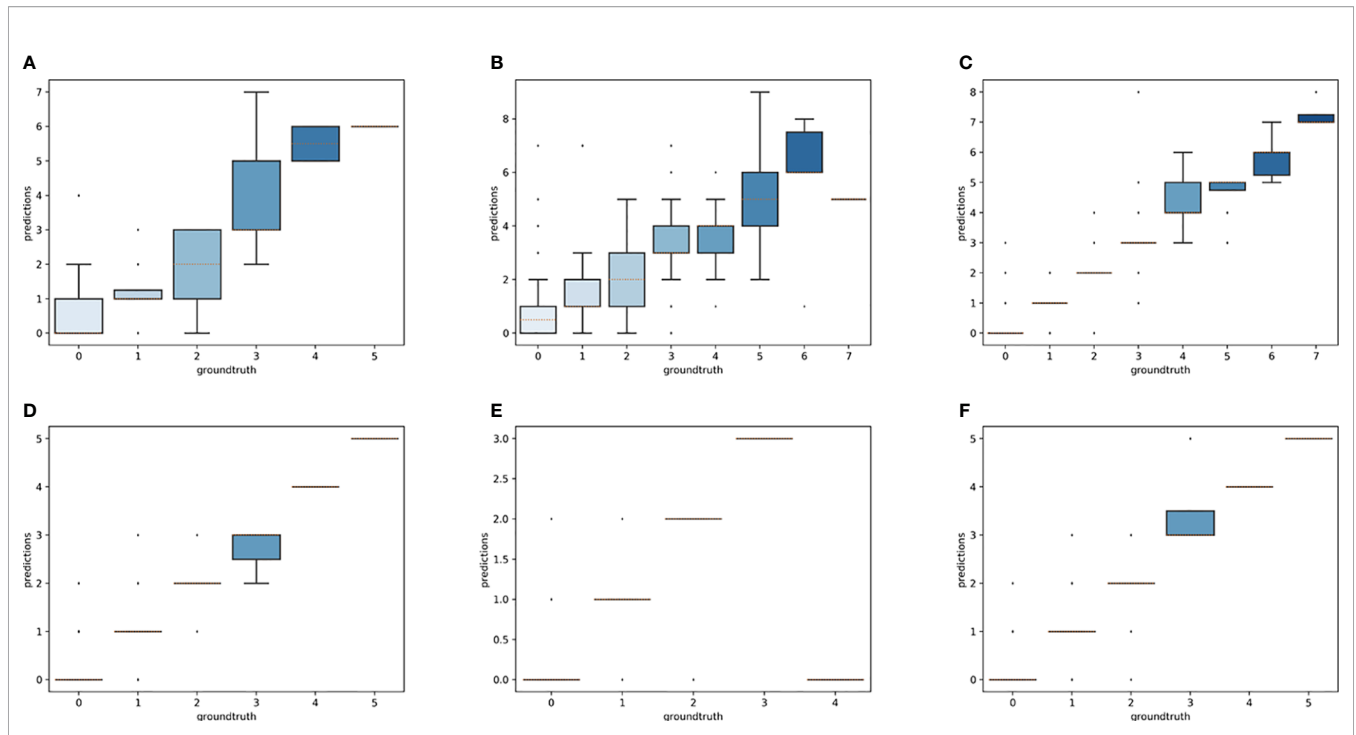


**FIGURE 7 |** Boxplot of the predicted counts vs. expected counts for each species. **(A)** *Anemone canadensis*; **(B)** *A. hepatica*; **(C)** *A. quinquefolia*; **(D)** *Trillium erectum*; **(E)** *T. grandiflorum*; **(F)** *T. undulatum*.

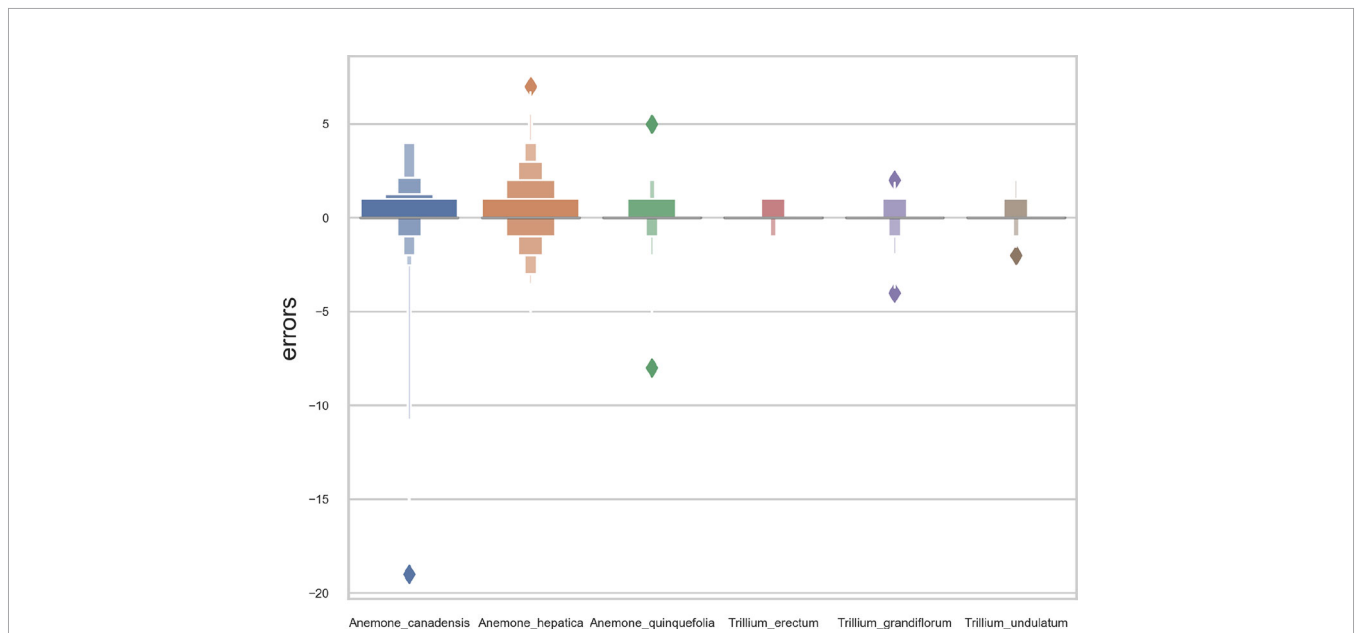


**FIGURE 8 |** Letter-value plot of the counting error for each species.

the machine learning community and is known to bring very significant improvements. The most simple yet very efficient method to build an ensemble is to train the same model several times but with a different random initialization of the parameters. Such strategy could be implemented in future work.

## DISCUSSION

Mask R-CNN models trained with human-annotated trait data were efficient and produced robust results. Our models worked well for both identifying and counting phenological features, but



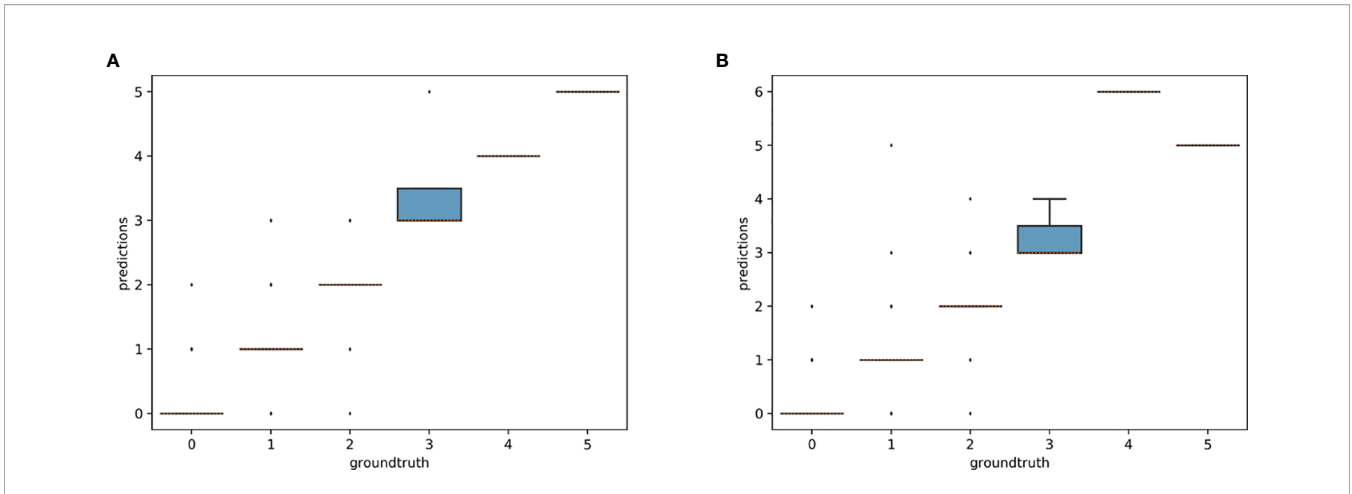


**FIGURE 9 |** Box-plots of the predicted counts vs. expected counts for *Trillium erectum*. **(A)** Model trained on *T. erectum* data; **(B)** model trained on *T. undulatum* and *T. grandiflorum*.

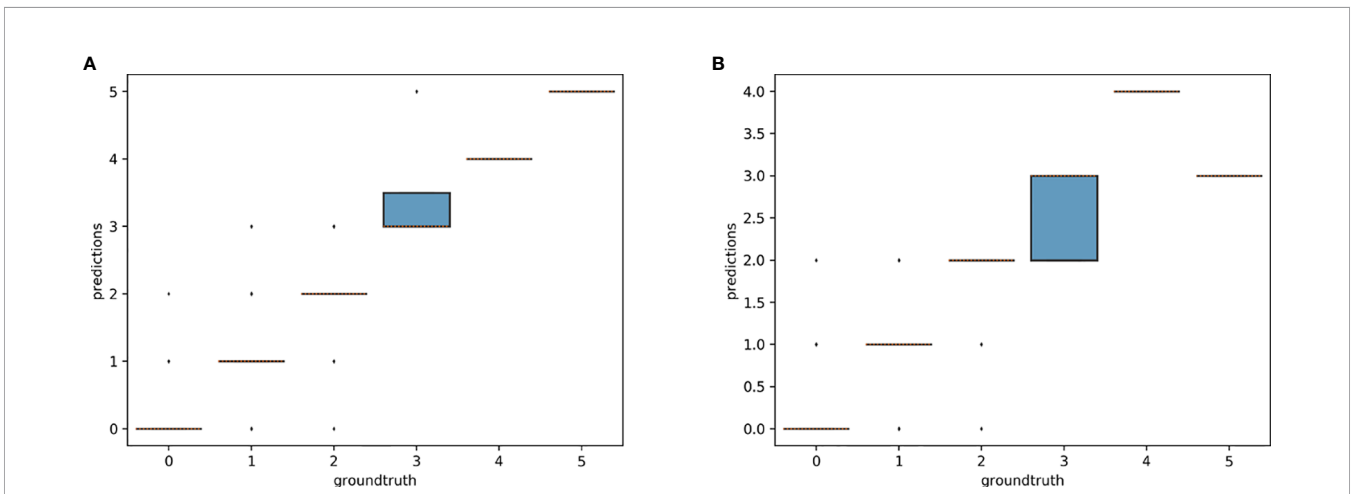


**FIGURE 10 |** Box-plots of predicted counts vs. observed counts for *Trillium undulatum*. **(A)** Model trained on *T. undulatum* data; **(B)** model trained on *T. erectum* and *T. grandiflorum*.

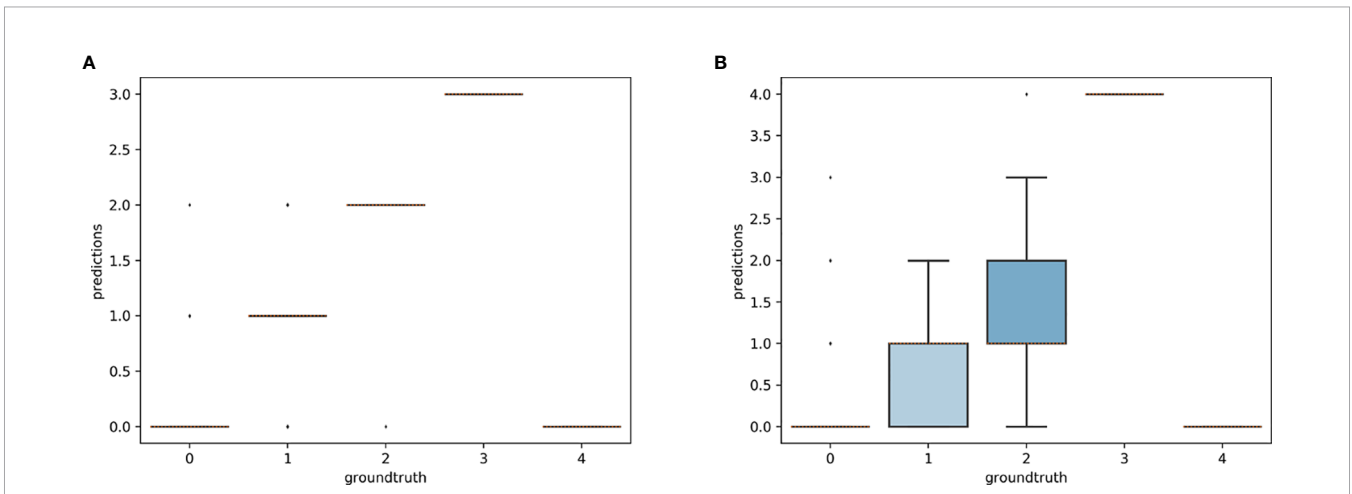


**FIGURE 11 |** Box-plots of predicted counts vs. expected counts for *Trillium grandiflorum*. **(A)** Model trained on *T. grandiflorum* data; **(B)** model trained on *T. erectum* and *T. undulatum*.

**TABLE 3** | Comparison of the counting error resulting from crowd-sourcing, deep learning and expert annotation—performance is measured by the Mean Absolute Error (MAE).

	Buds	Flowers	Fruits	All
Experts	0.009	0.027	0.073	0.036
Crowd-sourcing (isolated annotator)	0.526	0.487	0.314	0.442
Crowd-sourcing (average over all annotators)	0.418	0.405	0.243	0.355
Deep learning (model trained on all species)	<b>0.201</b>	<b>0.507</b>	<b>0.266</b>	<b>0.325</b>

**TABLE 4** | Comparison of the counting error resulting from crowd-sourcing, deep learning and expert annotation—performance is measured by R2 score.

	Buds	Flowers	Fruits	All
Experts	0.989	0.996	0.961	0.990
Crowd-sourcing (isolated annotator)	−2.969	0.758	0.306	0.555
Crowd-sourcing (average over all annotators)	−1.527	0.828	0.401	0.686
Deep learning (model trained on all species)	<b>0.141</b>	<b>0.750</b>	<b>0.329</b>	<b>0.707</b>

accuracy differed for buds, flowers, and fruits. Automated counts using Mask R-CNN models were more accurate than counts made by crowd-sourcers but not those of botanical experts. Finally, the Mask R-CNN model could be transferred to other species after being trained with data from reasonably close phylogenetic relatives, with relatively small impacts on counting accuracy.

## Point Masking With Minor Modification Is Efficient and Produces Robust Results

Recent efforts by Goëau et al. (2020) to segment and count reproductive structures used training data collected by botanical experts from 21 herbarium specimens of a single species (*S. tortuosus*). In our work, we applied Mask R-CNN to segment and count reproductive structures of six species, belonging to two different genera; accurate training data were derived from both botanical experts and crowd-sourcers using the *CrowdCurio* interface (Willis et al., 2017). Although Goëau et al. (2020) found that training data from point masks, like those generated from *CrowdCurio*, produced less accurate results than those derived from fully masked training data, obtaining the latter is time intensive and difficult to scale to large numbers of specimens. Whereas Goëau et al. (2020) produced three type of training data, “point masks” (produced from a 3 × 3-pixel box around a manual point marker); (ii) “partial masks” (extensions of point masks to include partial segmentation using the Otsu segmentation method (Otsu, 1979); and (iii) manually produced “full masks” of each reproductive structure, we only used modified partial masks (derived from point markers) with Mask R-CNN. These modified partial masks were scaled to the size of reproductive structures for each species and yielded high accuracy and efficiency for phenophase detection and counting. The scaling of our modified partial masks combined with the approximately circular shapes of the reproductive structures we studied likely led to the success of our approach. Our two-step workflow integrating expert-scored and crowd-sourced citizen science data with automated machine-learning models also is less

time-intensive and more scalable than a workflow requiring detailed polygon masks of structures for training.

## Feature Detection and Counting Accuracy Is High Across All Phenological Features

Lorieul et al. (2019) were the first to apply machine-learning to detect phenophases and developed a presence-absence model that could identify reproductive specimens with ≈96% accuracy. Their model was less accurate in detecting flowers or fruits (≈85 and ≈80% accuracy, respectively), and they did not consider buds. In contrast, we used Mask R-CNN to accurately identify the presence of each of the three reproductive stages (buds, flowers, or fruits) with ≥87% accuracy (Table 2). Moreover, a single globally-trained model was more efficient and had greater accuracy than multiple species-specific models (Figures 7 and 8). This points towards the possibility of developing a more streamlined workflow to accurately score phenophases of many different species simultaneously.

We also successfully estimated the relative abundance of each reproductive structure on a specimen with ≥90% accuracy (Table 2). Herbarium specimens can vary greatly in phenological state. Because different reproductive organs can co-exist at various times through plant development (and may not all be represented simultaneously on herbarium sheets), simply quantifying presence or absence of phenological structures limits inference about phenological state. In this regard, the Mask R-CNN model performed better on *Trillium*—with its large flowers and fruits, generally borne singly, and suspended on an elongate stalk—than on *Anemone*—with its small clusters of flowers on shorter stalks that are often pressed against a background of clustered leaves. The combination of smaller flowers, more complex morphology, and background “noise” on *Anemone* specimens (e.g., overlapping structures) likely made both model training and phenophase detection more prone to error. This result supports the recent hypotheses that successful application of machine-learning to phenophase assessment will be dependent on species-specific morphological details (Goëau et al., 2020). Along these lines, plant morphological trait databases could help facilitate the identification of suitable taxa to be analyzed with machine-learning methods.

Precise quantification of different reproductive structures, as demonstrated here, allows the determination of finer-scale phenophases (e.g., early flowering, peak flowering, peak fruiting). For this exercise, the lowest mean absolute error (MAE) was for bud counts, most likely due to the morphological consistency of buds and their rarity on specimens (Table 1). In contrast, MAE for counting flowers was significantly worse than for buds or fruits. We attribute this result to the greater number of flowers, ontogenetic variability in floral morphology, and variation in appearance of dried, pressed specimens.

Variation in appearance of reproductive features among dried and pressed specimens of a single species also could add complexity to automated detection of phenological features and merits further investigation. Perhaps more consequentially, large variation in the number of reproductive organs resulted in unbalanced datasets (Table 1). Numerous data augmentation

approaches can be implemented to improve comparisons and model selection for such data sets (e.g., Tyagi and Mittal, 2020), but these approaches have been used more frequently in classification or semantic segmentation (Chan et al., 2019) than in instance segmentation approaches such as we used here. Developing data augmentation approaches for instance segmentation would be a useful direction for future research. But even if collectors collect more flowering than non-flowering specimens, estimating the quantity of buds, flowers and fruits on any specimen is more informative than recording only their presence or absence.

## Botanical Experts Perform Better Than the Model

When considered in aggregate, the MAE for segmenting and counting all three phenophases using Mask R-CNN was lower than that of crowd-sourcers but still an order of magnitude higher than that of botanical experts (Tables 2 and 3). This result reinforces the suggestion that abundant and reliable expert data are essential for properly training and testing machine learning models (Brodrick et al., 2019). Additionally, it was evident in some cases that the precise detection of the phenological feature was quite inaccurate (Figure 2).

## Machines Can Apply Learning From One Species to Another, but Success Is Variable

For the first time to our knowledge, we have demonstrated that training data from related taxa can be used to detect and count phenological features of a species not represented in the training set (Figures 9–11). We limit our discussion of transferability here to species of *Trillium* owing to the ease of detecting and counting phenological features in this genus. Though in some cases species-specific models were highly transferable, model transferability varied greatly. For example, training on *Trillium undulatum* and testing on *T. erectum* (and vice-versa) was more accurate than when Mask R-CNN models trained with data from either of these species was applied to *T. grandiflorum*. *T. undulatum* and *T. erectum* are more similar morphologically than either is to *T. grandiflorum*, suggesting that morphological similarity may be a better guide for transferability success than phylogenetic relatedness (see Farmer and Schilling, 2002, for phylogenetic relationships of *Trillium*). This conclusion implies that transferability may be particularly challenging for clades that exhibit high morphological diversity and disparity among close relatives. The relationship between phylogenetic relatedness, morphological diversity, and model transferability should be investigated in future studies. The assessment of the sizes of the reproductive structures that could be captured by this type of approach should also be analyzed, to facilitate transferability.

## Future Directions

The presence of reproductive structures has been determined only infrequently during large-scale digitization and transcription efforts by the natural-history museums that generate this content. However, interest is growing rapidly in using

herbarium specimens for investigating historical changes in phenology and other ecological traits and processes. Our results have demonstrated success in automating the collection of large amounts of ecologically-relevant data from herbarium specimens. Together with controlled vocabularies and ontologies that are being developed to standardize these efforts (Yost et al., 2018), our two-stage workflow has promise for automating and harvesting phenological data from images in large virtual herbaria. In the long term, we would like to use the *CrowdCurio* workflow to generate reliable human-annotated data to further refine automated models for detecting phenological responses to climatic change from herbarium specimens across diverse clades and geographies. Finally, our results documenting transferability of machine-learning models from one species to another are preliminary, but promising. Although our universal model trained on all taxa performed better than our individual, species-specific models, there may be better ways to guide these efforts. For example, a hierarchy of individual models could yield more accurate results. These hierarchies might be phylogenetically organized (e.g., taxonomically by order, family, genus), leveraging information about shared morphologies common to related taxa and further governed by a set of rules that parse new specimens for phenophase detection based on their known taxonomic affinities (e.g., by genera). Similar approaches are already being applied today by corporations like Tesla Motors. Their automated driving suite uses different models for vehicle path prediction versus vehicle detection (Karpathy et al., 2014; Tesla, 2019).

## DATA AVAILABILITY STATEMENT

The images used and the datasets generated for this study are available from the Environmental Data Initiative doi: 10.6073/pasta/4d2e92ec343d716eb6ee3ee7cadec5ef.

## AUTHOR CONTRIBUTIONS

CD conceived the idea for the study. CD, DT, IB, and DP ran a pilot feasibility study to motivate the current project. DP and GL generated, organized, and assembled expert and non-expert crowd-sourced data to train the Mask R-CNN model. JX re-coded *CrowdCurio* for these experiments. JC, AJ, and PB conducted the analyses. CD, AJ, PB, JC, DP, and AE interpreted the results. CD wrote the first draft of the *Abstract*, *Introduction*, and *Discussion*. JC, AJ, and PB wrote the first draft of the *Methods* and *Results*. All authors contributed to the article and approved the submitted version.

## FUNDING

This study was funded as part of the New England Vascular Plant Project to CD (National Science Foundation (NSF)-DBI: EF1208835), NSF-DEB 1754584 to CD, DP, and AE, and by a

Climate Change Solutions Fund to CD and collaborating PIs in Brazil (R. Forzza, L. Freitas, C. El-Hani, GL, P. Rocha, N. Roque, and A. Amorim) from Harvard University. AE's participation in this project was supported by Harvard Forest. DP's contribution was supported by NSF-DBI: EF1208835. IB's contribution was supported by a NSF Postdoctoral Research Fellowship in Biology (NSF-DBI-1711936). The authors would also like to thank the French Agence Nationale de la Recherche (ANR), which has supported this research (ANR-17-ROSE-0003).

## REFERENCES

- Arteta, C., Lempitsky, V., and Zisserman, A. (2016). *Counting in the wild*. Cham: Springer International Publishing. 483–498.
- Boominathan, L., Kruthiventi, S. S., and Babu, R. V. (2016). Crowdnet: A deep convolutional network for dense crowd counting. *Proceedings of the 24th ACM International Conference on Multimedia*, Amsterdam, The Netherlands, 640–644.
- Brodrick, P. G., Davies, A. B., and Asner, G. P. (2019). Uncovering ecological patterns with convolutional neural networks. *Trends Ecol. Evol.* 34 (8), 734–745. doi: 10.1016/j.tree.2019.03.006
- Chan, R., Rottmann, M., Hüger, F., Schlicht, P., and Gottschalk, H. (2019). Application of decision rules for handling class imbalance in semantic segmentation. *bioRxiv* 1901.08394.
- Davis, C. C., Willis, C. G., Connolly, B., Kelly, C., and Ellison, A. M. (2015). Herbarium records are reliable sources of phenological change driven by climate and provide novel insights into species' phenological cueing mechanisms. *Am. J. Bot.* 102, 1599–1609. doi: 10.3732/ajb.1500237
- Falk, T., Mai, D., Bensch, R., Çiçek, Ö., Abdulkadir, A., Marrakchi, Y., et al. (2019). U-net: deep learning for cell counting, detection, and morphometry. *Nat. Methods* 16, 67–70. doi: 10.1038/s41592-018-0261-2
- Farmer, S., and Schilling, E. (2002). Phylogenetic analyses of Trilliaceae based on morphological and molecular data. *Syst. Bot.* 27, 674–692. doi: 10.1043/0363-6445-27.4.674
- Goëau, H., Mora-Fallas, A., Champ, J., Love, N., Mazer, S. J., Mata-Montero, E., et al. (2020). New fine-grained method for automated visual analysis of herbarium specimens: a case study for phenological data extraction. *Appl. Plant Sci.* 8 (6), e11368. doi: 10.1002/aps3.11368
- He, K., Zhang, X., Ren, S., and Sun, J. (2016). Deep residual learning for imagerecognition. *Proceedings of the IEEE Conference on Computer Vision and Pattern Recognition*, Las Vegas, NV, USA, 770–778.
- He, K., Gkioxari, G., Dollár, P., and Girshick, R. (2017). Mask R-CNN. *Proceedings of the IEEE International Conference on Computer Vision*, Honolulu, HI, USA, 2961–2969.
- Hedrick, B. P., Heberling, J. M., Meineke, E. K., Turner, K. G., Grassa, C. J., Park, D. S., et al. (2020). Digitization and the future of natural history collections. *BioScience* 70, 243–251. doi: 10.1093/biosci/biz163
- Heike, H., Wickham, H., and Kafadar, K. (2017). Letter-value plots: Boxplots for large data. *J. Comput. Graph. Stat.* 26, 469–477. doi: 10.1080/10618600.2017.1305277
- Karpathy, A., Toderici, G., Shetty, S., Leung, T., Sukthankar, R., and Li, F.-F. (2014). Large-scale video classification with convolutional neural networks. *2014 IEEE Conference on Computer Vision and Pattern Recognition*, Columbus, OH, USA, 1725–1732.
- Lin, T.-Y., Dollár, P., Girshick, R., He, K., Hariharan, B., and Belongie, S. (2017). Feature pyramid networks for object detection. *Proceedings of the IEEE Conference on Computer Vision and Pattern Recognition*, Honolulu, HI, USA, 2117–2125.
- Lorieul, T., Pearson, K. D., Ellwood, E. R., Goëau, H., Molino, J.-F., Sweeney, P. W., et al. (2019). Toward a large-scale and deep phenological stage annotation of herbarium specimens: Case studies from temperate, tropical, and equatorial floras. *Appl. Plant Sci.* 7, e01233. doi: 10.1002/aps3.1233
- Love, N. L. R., Park, I. W., and Mazer, S. J. (2019). A new phenological metric for use in pheno-climatic models: A case study using herbarium specimens of *streptanthus tortuosus*. *Appl. Plant Sci.* 7, e11276. doi: 10.1002/aps3.11276

## ACKNOWLEDGMENTS

The authors are grateful to Inria Sophia Antipolis—Méditerranée “NEF” computation platform for providing resources and support. The authors acknowledge iDigBio's Phenology and Machine Learning Workshop (1/2019), which helped to stimulate this collaboration. The authors are grateful for the efforts of citizen scientists that helped generate data and the many collectors and curators of plant specimens that have made this research possible.

- Massa, F., and Girshick, R. (2018). maskrcnn-benchmark: Fast, modular reference implementation of instance segmentation and object detection algorithms in pytorch.
- Meineke, E. K., Davis, C. C., and Davies, T. J. (2018). The unrealized potential of herbaria for global change biology. *Ecol. Monogr.* 88, 505–525. doi: 10.1002/ecm.1307
- Meineke, E. K., Davies, T. J., Daru, B. H., and Davis, C. C. (2019). Biological collections for understanding biodiversity in the Anthropocene. *Philos. Trans. R. Soc. London B* 374, 20170386. doi: 10.1098/rstb.2017.0386
- Miller-Rushing, A. J., Primack, R. B., Primack, D., and Mukunda, S. (2006). Photographs and herbarium specimens as tools to document phenological changes in response to global warming. *Am. J. Bot.* 93, 1667–1674. doi: 10.3732/ajb.93.11.1667
- Nelson, G., and Ellis, S. (2019). The history and impact of digitization and digital data mobilization on biodiversity research. *Philos. Trans. R. Soc. B* 374, 20170391. doi: 10.1098/rstb.2017.0391
- Otsu, N. (1979). A threshold selection method from gray-level histograms. *IEEE Trans. Syst. Man Cybern.* 9, 62–66. doi: 10.1109/TSMC.1979.4310076
- Park, D., Williams, A., Law, E., Ellison, A., and Davis, C. (2018). Assessing plant phenological patterns in the eastern United States over the last 120 years. doi: 10.6073/pasta/f6afa728bb5edfd79f458d7d5e23f559
- Park, D. S., Breckheimer, I., Williams, A. C., Law, E., Ellison, A. M., and Davis, C. C. (2019). Herbarium specimens reveal substantial and unexpected variation in phenological sensitivity across the eastern United States. *Philos. Trans. R. Soc. B* 374, 20170394. doi: 10.1098/rstb.2017.0394
- Paszke, A., Gross, S., Massa, F., Lerer, A., Bradbury, J., Chanan, G., et al. (2019). Pytorch: An imperative style, high-performance deep learning library. *Advances in Neural Information Processing System* 32. Vancouver, BC, Canada, 8024–8035.
- Pearson, K. D., Nelson, G., Aronson, M. F. J., Bonnet, P., Brenskelle, L., Davis, C. C., et al. (2020). Machine learning using digitized herbarium specimens to advance phenological research. *BioScience* 70 (7), 610–620. doi: 10.1093/biosci/biaa044
- Pearson, K. D. (2019). A new method and insights for estimating phenological events from herbarium specimens. *Appl. Plant Sci.* 7, e01224. doi: 10.1002/aps3.1224
- Primack, D., Imbres, C., Primack, R. B., Miller-Rushing, A. J., and Del Tredici, P. (2004). Herbarium specimens demonstrate earlier flowering times in response to warming in Boston. *Am. J. Bot.* 91, 1260–1264. doi: 10.3732/ajb.91.8.1260
- Ronneberger, O., Fischer, P., and Brox, T. (2015) U-Net: Convolutional Networks for Biomedical Image Segmentation. In: Navab, N., Hornegger, J., Wells, W., and Frangi, A. (eds) *Medical Image Computing and Computer-Assisted Intervention – MICCAI 2015*. MICCAI 2015. Lecture Notes in Computer Science, vol 9351. Cham: Springer, 234–241.
- Seguí, S., Pujol, O., and Vitria, J. (2015). Learning to count with deep object features. *Proceedings of the IEEE Conference on Computer Vision and Pattern Recognition Workshops*, Boston, MA, USA, 90–96.
- Sweeney, P. W., Starly, B., Morris, P. J., Xu, Y., Jones, A., Radhakrishnan, S., et al. (2018). Large-scale digitization of herbarium specimens: Development and usage of an automated, high-throughput conveyor system. *Taxon* 67, 165–178. doi: 10.12705/671.9
- Tesla, (2019). *Tesla Autonomy Day 2019 - Full Self-Driving Autopilot - Complete Investor Conference Event*. <https://www.youtube.com/watch?v=-b041NXGPZ8>
- Thiers, B. (2017). Index Herbariorum: a global directory of public herbaria and associated staff. New York Botanical Garden's Virtual Herbarium. <http://sweetgum.nybg.org/ih/>. [6/5/2020]

- Tyagi, S., and Mittal, S. (2020). "Sampling approaches for imbalanced data classification problem in machine learning," in *Proceedings of ICRIC 2019. Lecture Notes in Electrical Engineering*, vol. 597. (Cham, Switzerland: Springer), 209–221.
- Wang, C., Zhang, H., Yang, L., Liu, S., and Cao, X. (2015). Deep people counting in extremely dense crowds. *Proceedings of the 23rd ACM International Conference on Multimedia*, Shanghai, China, 1299–1302.
- Williams, A. C., Goh, J., Willis, C. G., Ellison, A. M., Brusuelas, J. H., Davis, C. C., et al. (2017). "Deja vu: Characterizing worker reliability using task consistency," in *Proceedings of the Fifth Conference on Human Computation and Crowdsourcing [HCOMP 2017]* (Menlo Park, CA, USA: Association for the Advancement of Artificial Intelligence), 197–205.
- Willis, C. G., Ellwood, E. R., Primack, R. B., Davis, C. C., Pearson, K. D., Gallinat, A. S., et al. (2017). Old plants, new tricks: phenological research using herbarium specimens. *Trends Ecol. Evol.* 32, 531–546. doi: 10.1016/j.tree.2017.03.015
- Wolkovich, E. M., Cook, B.II, and Davies, T. J. (2014). Progress towards an interdisciplinary science of plant phenology: building predictions across space, time and species diversity. *New Phytol.* 201, 1156–1162. doi: 10.1111/nph.12599
- Yost, J. M., Sweeney, P. W., Gilbert, E., Nelson, G., Guralnick, R., Gallinat, A. S., et al. (2018). Digitization protocol for scoring reproductive phenology from herbarium specimens of seed plants. *Appl. Plant Sci.* 6, e1022. doi: 10.1002/aps3.1022
- Zhang, C., Li, H., Wang, X., and Yang, X. (2015). Cross-scene crowd counting via deep convolutional neural networks. *Proceedings of the IEEE Conference on Computer Vision and Pattern Recognition*, Boston, MA, USA, 833–841.

**Conflict of Interest:** The authors declare that the research was conducted in the absence of any commercial or financial relationships that could be construed as a potential conflict of interest.

Copyright © 2020 Davis, Champ, Park, Breckheimer, Lyra, Xie, Joly, Tarapore, Ellison and Bonnet. This is an open-access article distributed under the terms of the Creative Commons Attribution License (CC BY). The use, distribution or reproduction in other forums is permitted, provided the original author(s) and the copyright owner(s) are credited and that the original publication in this journal is cited, in accordance with accepted academic practice. No use, distribution or reproduction is permitted which does not comply with these terms.